

Dual RNA-seq reveals no plastic transcriptional response of the coccidian parasite *Eimeria falciformis* to host immune defenses

3

4Totta Ehret^{1,2}, Simone Spork¹, Christoph Dieterich³, Richard Lucius¹, Emanuel Heitlinger^{1,4,C}

5

61. Institute of Biology, Molecular Parasitology, Humboldt-Universität zu Berlin

7Philippstr. 13, Haus 14, 10115 Berlin, Germany

82. FG16 - Mycotic and parasitic agents and mycobacteria, Robert Koch Institute, Berlin,

9Germany

103. University Hospital Heidelberg - German Center for Cardiovascular Research (DZHK),

11Analysezentrum III, Im Neuenheimer Feld 669, 69120 Heidelberg, Germany

124. Leibniz Institute for Zoo and Wildlife Research, Research Group Ecology and Evolution of

13Parasite Host Interactions, Alfred-Kowalke-Str. 17, 10315, Berlin, Germany

14

15TE: totta.kasemo@gmail.com

16SS: sporksim@hu-berlin.de

17CD: christoph.dieterich@uni-heidelberg.de

18RL: richard.lucius@hu-berlin.de

19EH: emanuel.heitlinger@hu-berlin.de, heitlinger@izw-berlin.de

20C. Corresponding author

21

22

23

24 **ABSTRACT**

25 **Background:** Parasites can either respond to differences in immune defenses that exist
26 between individual hosts plastically or, alternatively, follow a genetically canalized (“hard
27 wired”) program of infection. Assuming that large-scale functional plasticity would be
28 discernible in the parasite transcriptome we have performed a dual RNA-seq study of the full
29 lifecycle of *Eimeria falciformis* using infected mice with different immune status (e.g. naïve
30 versus immune animals) as models for coccidian infections.

31 **Results:** We compared parasite and host transcriptomes (dual transcriptome) between naïve
32 and challenge infected mice, as well as between immune competent and immune deficient
33 ones. Mice with different immune competence show transcriptional differences as well as
34 differences in parasite reproduction (oocyst shedding). Broad gene categories represented by
35 differently abundant host genes indicate enrichments for immune reaction and tissue repair
36 functions. More specifically, TGF-beta, EGF, TNF and IL-1 and IL-6 are examples of functional
37 annotations represented differently depending on host immune status. Much in contrast,
38 parasite transcriptomes were neither different between *Coccidia* isolated from immune
39 competent and immune deficient mice, nor between those harvested from naïve and challenge
40 infected mice. Instead, parasite transcriptomes have distinct profiles early and late in infection,
41 characterized largely by biosynthesis or motility associated functional gene groups,
42 respectively. Extracellular sporozoite and oocyst stages showed distinct transcriptional profiles
43 and sporozoite transcriptomes were found enriched for species specific genes and likely
44 pathogenicity factors.

45 **Conclusion:** We propose that the niche and host-specific parasite *E. falciformis* uses a
46 genetically canalized program of infection. This program is likely fixed in an evolutionary

process rather than employing phenotypic plasticity to interact with its host. In turn this might (negatively) influence the ability of the parasite to use different host species and (positively or negatively) influence its evolutionary potential for adaptation to different hosts or niches.

50

51 Keywords

Phenotypic plasticity, Parasite lifecycle, Transcriptional plasticity, Apicomplexa, Dual RNA-seq, Dual transcriptomics, Coccidia

54

55 BACKGROUND

The term plasticity describes the ability of genetically identical organisms to display variable phenotypes, e.g., via different developmental or metabolic programs. So called reaction norms govern how a particular genotype is translated into a phenotype depending on environmental stimuli [1]. The presence of predators is known to alter, e.g., developmental programs of genetically identical prey animals to produce different phenotypes (reviewed in [2]). Infections by pathogens are known to alter host phenotypes: in fact all non-constitutive immune reactions can be regarded as a manifestation of plasticity [3]. Hence, to understand the outcomes of parasitic infections and host-parasite interactions the concept of plasticity is useful.

64

The reciprocal effect of the within-host environment on parasite phenotypes, i.e. plasticity, is less studied, especially in parasites of animals. For many parasite species it remains unclear whether differences in pathology are due to parasites' genotypic or phenotypic (plastic) differences, the latter resulting from host-parasite interactions, e.g., host immune responses. An exception are Nematode infections (reviewed by [4]), in which for example worm length [5]

and other aspects of morphology [6], or developmental timing [7] has been shown to vary with host genotype. However, it is unclear to which extent such differences are passively imposed on the parasite or whether they are responses with functional relevance as an adaptation of the parasite expressing observed phenotypes.

Only recently have transcriptomes been used to investigate plasticity in “infection programs”, which parasites induce as a response to host signals. Since gene expression is orchestrated by the genetic makeup of an organism, plasticity in transcription – when it occurs – is likely to be an adaptation which allows the parasite to react on host stimuli and to produce an altered phenotype. We here distinguish between such plastic (responsive) transcription programs and what is sometimes referred to phenotypic plasticity, which then is a “passive” phenotypic change imposed on the parasite without being controlled at the transcriptional level. A perceivable example could be reduced growth due to “mechanical” impact, e.g., limited space. In a Nematode, the presence of phenotypic plasticity has for example been shown to lack a transcriptional basis [8], and can therefore be regarded “passive”. In contrast, unicellular *Entamoeba* spp. infections of variable pathogenicity (i.e. phenotypic plasticity) manifested also in transcriptional differences under various in vitro conditions [9]. Among apicomplexan parasites, different infection programs with distinct transcriptional profiles have been proposed: in *Plasmodium* spp., the parasite’s transcriptome is distinct in different mouse genotypes (BALB/c and C57BL/6) and tissues within one genotype [10], hence demonstrating the capability for plasticity in this parasite. Similarly and even more closely related to *Eimeria* spp., the coccidian *Toxoplasma gondii* forms dormant tissue cysts (bradyzoites), a process induced by and depending on the host environment [11], and involving large changes in parasite

transcriptomes [12]. In addition, *T. gondii* is capable of infecting all studied warm-blooded vertebrates and all nucleated cells in those animals [13] suggesting parasite plasticity in different host environments also in the tachyzoite stage.

E. falciformis is an intracellular parasite in the phylum Apicomplexa, which comprises more than 4000 described species [14]. Prominent pathogens of humans are found in this phylum, such as *T. gondii*, the causative agent of toxoplasmosis, *Plasmodium* spp., causing malaria, and *Cryptosporidium* spp., which cause cryptosporidiosis. Coccidiosis is a disease of livestock and wildlife caused by coccidian parasites which are dominated by > 1,800 species of *Eimeria* [14]. The genus is best known for several species which are problematic for the poultry industry [15]. *E. falciformis* naturally infects wild and laboratory *Mus musculus*, and its genome is sequenced and annotated making it a useful model for studying *Eimeria* spp. [16]. The parasite has its niche in the cecum and upper part of colon, mainly in the cells of the crypts [17,18]. This monoxenous parasite goes through asexual (schizogony) and sexual reproduction, which results in the host releasing high numbers of oocysts approximately between day six and 14 after infection. When a mouse ingests *E. falciformis* oocysts, one sporulated oocyst releases eight infective sporozoites inside the host, which infect epithelial crypt cells. Within the epithelium, merozoite stages form in several rounds of asexual reproduction, followed by gamete formation and sexual reproduction, within the same host. Schizogony takes place approximately until day six and then gametes form and sexual reproduction takes place, resulting in unsporulated oocyst shedding. Schizogony is not completely synchronous; the exact number of schizogony cycles is unclear and could vary naturally [17,19]. There is evidence for a genetic predisposition of *Eimeria* spp. to perform

different numbers of schizogony cycles, as parasites can be selected to become “precocious”, completing the lifecycle faster with a reduced number of schizogony cycles [20,21]. Such results have not been obtained for *E. falciformis*, and similarly, it is not known whether such parasite programs are plastic and can also be triggered by exogenous stimuli, such as host immune responses.

Eimeria spp. generally induce host protection against reinfection [19,22–24] and T-cells seem to play a major role [25,26]. In responses to *E. falciformis* infection of laboratory mice, IFN γ is upregulated [18]. In an IFN γ -deficient mouse host model which displays larger weight losses and intestinal pathology but also lower oocyst output, the wild-type phenotype was recovered by blocking IL-17A and IL-22 signaling [27]. These studies demonstrate that adaptive immunity clearly plays a role in limiting the reproductive success of *Eimeria* spp. infection, but effects on the parasite, apart from reproductive output, remain poorly understood. It is an open question whether the parasite is passively impacted or responds, e.g., via changes in its transcriptome, to changes in the host immune response.

We used a “dual RNA-seq” approach, i.e., we simultaneously assessed the transcriptomes of host and parasite in biological samples containing both species [28–32]. Applying this to an infection of *E. falciformis* in the mouse, we produced host and parasite transcriptomes from the same samples, tissue, and time-points. We describe and analyze host and parasite mRNA profiles at several time-points post infection and contrast transcriptomes of naïve and challenge infected wild-type mice to hosts with strong deficiency in adaptive immune responses. This approach allows us to screen transcriptional changes which may be involved

139in host-parasite interactions for plasticity to alterations in the host immune system. We
140hypothesize that changes in the parasite transcriptome would be indicative of a plastic
141response allowing for functionally altered infection programs.

142

143RESULTS & DISCUSSION

144Immune competent hosts induce protective immunity against *E. falciformis* 145infection

146To investigate *E. falciformis* development throughout the lifecycle in a natural mouse host
147(NMRI mice) dual transcriptomes were produced at 3, 5, and 7 days post infection (dpi). We
148also investigated parasite development and transcriptomes in a mouse strain which is severely
149limited in adaptive immune responses (*Rag1*^{-/-}; “immunocompromised” hereafter) with *Rag1*^{-/-}
150and the respective isogenic background strain (C57BL/6 as control) at day 5 post infection. To
151further elucidate host immune responses and parasite sensitivity to host immunity, we also
152challenge infected all mouse groups (i.e. infected after recovery of a first infection; see
153Methods) and sampled at the same time-points as in naïve mice.

154

155Infections showed drastically decreased oocyst output (Figure 1A and B) in immune competent
156hosts undergoing a second, challenge infection compared to naïve animals infected for the first
157time (Mann–Whitney test, in NMRI, n = 12, U = 32, p = 0.004; in C57BL/6, n = 24, U = 111, p =
1580.008). Similarly, a strong reduction of parasite 18S rRNA in the challenge infection down to
1593.5% of the amount measured in naïve hosts was detected in reverse transcription quantitative
160PCR (RT-qPCR) in NMRI hosts (Figure 1C). The model inferring this had a good fit ($R^2 = 0.94$)
161and the change of the intercept for challenged compared to naïve hosts was highly significant

162($t = -6.71$; $p < 0.001$). Differences in the slope were not significant ($t = -1.522$; $p = 0.15$),
 163indicating that the amount of parasite material on 3 days post infection is sufficient to explain a
 164linear increase until 7 days post infection. Overall this data is in line with the strong reduction of
 165oocyst shedding seen in challenge infected immune competent mice, and suggests that the
 166host immune defense disturbs the parasite during gamogony or oocyst formation. Further,
 167these results do not give support to drastic changes in the parasite's "infection program" and
 168rather suggests a non-plastic lifecycle progression.

169
 170In contrast, in immune deficient mice no significant difference in parasite reproductive success
 171(Figure 1A) was observed between naïve and challenge infection (Mann–Whitney test; $n = 24$,
 172 $U = 96$, $p = 0.10$). Both in the immunocompromised and immune competent animals, however,
 173all mice had cleared the infection by day 14. We thereby note that *E. falciformis* infection is
 174self-limiting also in mice without mature T- and B-cells, however with a delayed peak of oocyst
 175shedding in immune deficient hosts (Figure 1B).

176

177 **Parasite and host dual transcriptomes can be assessed in parallel**

178We found the increase in parasite numbers over time after infection to also be reflected by the
 179proportion of *E. falciformis* mRNAs sequenced in the combined pool of transcripts from host
 180and parasite (for NRMI mice in Figure 1D). Using mRNA from infected cecum epithelium we
 181demonstrate that even early in infection (3 dpi, during early asexual reproduction) there is
 182sufficient parasite material to detect parasite mRNAs in the pool including host mRNAs, and to
 183quantify individual host and parasite mRNA abundance (Table 1). The number of total (host +

184parasite) read mappings for individual replicates ranged from 25,362,739 (sample
185Rag_1stInf_0dpi_rep1) to 230,773,955 (NMRI_2ndInf_5dpi_rep1).

186
187We did not detect bias in overall mRNA abundance patterns induced by, e.g., sequencing
188technologies (batch effects) using a multivariate technique (multidimensional scaling). Efficient
189normalization was confirmed in that samples with large differences in parasite read proportions
190show similar transcriptome signatures (Figure S1). This normalization also resulted in
191unimodal distributions of read numbers (Figure S2) in agreement with negative binomial
192distributions assumed for statistical modeling and testing.

193
194Remarkably, on day 7 post infection, the day before oocyst shedding peaks, samples from
195infected naïve mouse epithelium contained 77% and 92% parasite mRNA, i.e., drastically more
196mRNA from the parasite than from the host (Figure 1D and Table 1). Our transcriptomes for
197these late infection samples are in agreement with previously published microarray data from
198mice infected with *E. falciformis* [18], as log₂ fold-changes at our 7 days post infection versus
199controls correlated strongly – for given mRNAs – with log₂ fold changes at 6 days post
200infection versus controls in that study (Spearman's $\sigma = 0.72$, $n = 9017$, $p < 0.001$; Figure S3).
201Considering both biological differences in the experiments, such as exact time-points for
202sampling, and technical differences between the two methods, this correlation confirms the
203adequacy of using dual RNA-seq for assessing the host transcriptome in the presence of large
204proportions of parasite mRNA. Below, we first describe changes in the mouse transcriptome
205and suggest possible mechanisms at play. Variance in host transcriptome changes upon

infection constitutes a potential environmental stimulus for parasites to react on, as addressed later.

208

The mouse transcriptome undergoes large changes upon *E. falciformis* infection

211

We here show that upon infection with *E. falciformis*, which induces weight loss (Figure S4) and intestinal pathology in mice, the host transcriptome undergoes drastic changes affecting more than 3000 individual mRNA profiles significantly (edgeR; glm likelihood-ratio tests corrected for multiple testing, false discovery rate [FDR] < 0.01, see below). Statistical testing for differential abundance between infected and uninfected mice revealed that differences in mRNA abundance were more pronounced (both in magnitude and number of genes affected) at the two later time-points post infection (Table 2 and Figure 2A). 325 mRNAs were differently abundant (FDR < 0.01) between controls and 3 dpi, 1,804 mRNAs between controls and 5 dpi, and 2,711 mRNAs between controls and 7 dpi. This leads to a combined set of 3,453 transcripts responding to infection. Differentially abundant mRNAs early in infection (3 and 5 dpi) were not a mere subset of genes differentially abundant later in infection (7 dpi; Figure 2A), which would be the case if the same genes were regulated throughout infection. Instead, the transcriptional profile of the mouse changes more fundamentally with different genes varying in abundance late compared to early in infection.

226

To further analyze the distinct responses early and late in infection, we performed hierarchical clustering on transcript abundance patterns at different time-points post infection (Figure 2B).

229 Three main sample clusters formed (dendrogram indicating similarities between columns at top
230 of Figure 2B). Immune deficient *Rag1*^{-/-} mice, including infected *Rag1*^{-/-} samples, show an
231 expression pattern most similar to uninfected samples. This similarity between infected and
232 non-infected *Rag1*^{-/-} samples confirms the immune deficiency phenotype; a failure to react to
233 infection in these mice, and suggests a strong influence of adaptive immune responses on
234 overall transcriptional responses. Surprisingly, these patterns indicate that innate immune
235 responses and other B- and T-cell independent processes play detectable though relatively
236 small roles (mouse gene cluster 4; Mm-cluster hereafter, Figure 2B) in shaping the mouse
237 transcriptome upon *E. falciformis* infection.

238

239 ***Responses to parasite infection differ between immunocompromised and immune*** 240 ***competent mice***

241 The self-limiting nature of *E. falciformis* infection and host resistance to reinfection ([33] and
242 Figure 1A) makes it interesting to analyze transcriptomes of immune competent hosts in depth.
243 On 3 and 5 days post infection, mRNAs of two clusters of genes have overall high abundance
244 in samples of all immune competent infected animals (Mm-clusters 1 and 2). Other mRNAs
245 (Mm-clusters 3 and 4) show lowered abundance in all those infected samples.

246

247 Gene Ontology (GO) terms enriched among the mRNAs which become more abundant only
248 early in infection (Mm-clusters 1 and 2) are, e.g., “stem cell population maintenance”, “mRNA
249 processing”, and “cell cycle G2/M transition”, indicating tissue remodeling in the epithelium. In
250 addition, terms such as “regulation of response to food” are enriched (Table S1). This is
251 interesting since weight losses and malnutrition are generally common during parasitic

infections [34, 35], also in *Eimeria* spp. infections [36-38], and weight loss was also seen in the present study (Figure S4).

Genes whose mRNA levels decreased in abundance upon infection (Mm-clusters 3 and 4) indicate induction of IL-1 and IL-6, which are involved in inflammation, including T- and B-cell recruitment and maturation, and broad acute phase immune responses (Table S1). IL-6 has also been shown to support tissue repair and inhibit apoptosis after epithelial wounding [39]. In addition, IL-6 is linked to Th17 responses [40] which are known to play an important role in responses to *E. falciformis* [27]. Further terms indicate a regulation of transforming growth factor- β (TGF β) which is important for wound healing in intestinal epithelium [41], epidermal growth factor (EGF) and tumor necrosis factor (TNF), which regulate proliferation of epithelial cells and inhibit apoptosis in epithelial cells [42,43]. Inhibition of Notch signaling, which is also highlighted by GO terms, has been shown to alter the composition of cell-types in the epithelium towards Paneth and Goblet-like cells [44].

Although speculative, several of the GO terms (e.g. “calcineurin-NFAT signaling cascade”, “Inositol-phosphate mediated signaling”, “Notch receptor processing” in addition to those mentioned above) annotated to genes whose mRNA levels change in abundance upon early infection (Mm-cluster 3 and 4) can be linked to explain fundamental mechanisms. Inositol signaling can lead to release of calcium and calcineurin-dependent translocation of NFAT to the nucleus; and there to activation of NFAT target genes in T-cells, but also many other cell types [45]. In addition, changes in the host epithelium do take place when cells are invaded by, e.g., *E. falciformis*, but also generally by pathogens, and this is reflected in the stem-cell and

cell cycle-related GO terms described above for Mm-clusters 1 and 2. Further investigation of the role of the processes and molecules highlighted here will contribute to better understanding for epithelial responses to intestinal intracellular parasitic infection. Interestingly, in T- and B-cell deficient hosts, the same four groups of genes described above (Mm-clusters 1-4, Figure 2B), which are responsible for these dominating responses in immune competent hosts show no differences between infected and non-infected immune deficient animals.

281

Adaptive immune responses characterize late infection

Pronounced transcriptional changes in the mouse host occur late in infection in immune competent animals (Table 2 and Mm-cluster 5 in Figure 2B). Annotated processes and functions (GO terms) for genes with increased abundance at 7 days post infection reflect the expected onset of an adaptive immune response (Table S1). As late as 5 days post infection, genes responsible for these enrichments are still low on mRNA abundance. This confirms a strong induction of immune responses, particularly adaptive immune responses, between 5 and 7 days post infection. This result is well in line with previously described immune responses to infection with *Eimeria* spp. [23–27].

291

Protective responses occur earlier in challenge infected than in naïve hosts

Transcriptomes from three samples from early and late challenge infection show the same distinct profile of elevated mRNA abundance at 3, 5 and 7 days post infection (Mm-cluster 6, Figure 2B). The underlying mRNAs are highly enriched for GO terms for RNA processing, e.g., splicing, which indicated post-transcriptional regulation. In addition, terms for histone and chromatin modification are enriched (Table S1). This, along with less oocyst shedding during

challenge infection, suggests that protective immune responses in challenge infected animals are regulated both at the transcriptional and post-transcriptional level. The high abundance of these mRNAs at different time-points post infection in wild-type hosts (NMRI) further indicates that protective immunity is similar at these time-points. Possibly, induction and chronologic differences in challenge infected animals occur before 3 days post infection. The completely cleared infection in some samples (Table 1; and unexpected clustering of e.g. NMRI_2ndInf_7dpi_rep2), apart from clearly demonstrating protection, also supports an early timing of this response upon challenge infection. However, the distinct shared profile at the investigated time-points (days 3, 5, and 7) does show that the protective response is still detectable at the transcriptional level several days after the challenge.

308

A framework to interpret *E. falciformis* transcriptomes is provided by orthologues in the Coccidia *E. tenella* and *T. gondii*

To establish *E. falciformis* as a model for coccidian parasites, transcriptome profiles of orthologue genes from closely related parasites can help to draw parallels between lifecycle stages. This can be informative in predicting gene function and in analyzing evolutionary forces acting on the different lifecycle stages. Therefore, we performed correlation analysis between our *E. falciformis* transcriptome and RNA-seq transcriptomes from closely related parasites at corresponding stages of their lifecycles. Two datasets for the economically important chicken parasite *E. tenella* [46,47] and one dataset of the model apicomplexan parasite *T. gondii* [48] were included. The latter was used because it is to date the only available dataset for the complete in vivo lifecycle of *T. gondii* (including stages in the definitive cat host), and therefore compares well with our data.

321

322 For all samples from these studies and our data, abundances of orthologous genes were
323 correlated and Spearman's coefficient was compared (Figure 3). With the exception of
324 sporozoites (see below), transcriptomes tend to be more strongly correlated (similar) between
325 corresponding lifecycle stages of different parasite species than between stages in the same
326 parasite species.

327

328 Orthologues in *E. tenella* and *E. falciformis* gamete stages (purified gametocytes and 7 dpi
329 intestinal samples, respectively) are highly correlated in their expression across the two
330 species, indicating conserved gene sets orchestrating sexual replication of the two parasites.
331 Similarly, transcriptomes of *E. tenella* merozoites from both independent studies of that
332 parasite are most similar to early *E. falciformis* samples, indicating similarity also during
333 asexual reproduction. *E. falciformis* unsporulated oocyst transcriptomes share the highest
334 similarity with those of unsporulated *E. tenella* oocysts.

335

336 *E. falciformis* sporozoites transcriptome profiles are more similar to *E. falciformis* early infection
337 samples than to sporozoite transcriptomes of *E. tenella* orthologues. Similarities between
338 sporozoites and early infection stages could be explained by similar biological processes,
339 especially host cell invasion (and reinvasion by merozoites), being prepared or performed.
340 Sporozoites are the only lifecycle stages in which orthologue mRNA abundance patterns show
341 such dissimilarities to *E. tenella* and this might indicate a higher species specificity of the
342 genes and processes in this invasive stage. This could be a result of virulence factors being
343 expressed in this stage, which are known to undergo rapid gene family expansion, as seen in

SAGs in *E. falciformis* [16], *T. gondii* [49], *Neospora caninum* [50], and other *Eimeria* spp. [46], or var genes in *Plasmodium falciparum* [51].

346

Below we provide a detailed description of the *E. falciformis* transcriptome, including a discussion of genes which have been shown to be important in closely related parasites such as *E. tenella* and *T. gondii*.

350

Overall transcriptional changes in the lifecycle of *E. falciformis*

Similar to the host transcriptome, differences in parasite mRNA abundance were mostly observed between late and early infection. Between 3 and 5 dpi 103 mRNAs were differently abundant (edgeR likelihood ratio tests on glms; FDR < 0.01), whereas between 3 and 7 dpi 1399 mRNAs, and between 5 and 7 dpi 2084 mRNAs were differentially abundant (Figure 4A). Hierarchical clustering did not group samples from 3 and 5 days distinctively and we thus refer to these as "early infection" and 7 dpi as "late infection". Distinct abundance differences define early infection (parasite gene cluster 6, "Ef-cluster" hereafter, Figure 4B). At those time-points asexual reproduction takes place [17,19]. Two separate clusters define late infection (7 dpi, Ef-clusters 2 and 7) in which we assume gametocytes to be present due to the peak of oocyst shedding one day later (Figure 1A) [17] and similarity of these transcriptomes with purified *E. tenella* gametocytes (Figure 3). The extracellular stages, sporozoites (Ef-cluster 4) and unsporulated oocysts (Ef-clusters 1 and 5) are clearly distinct by high mRNA abundance. In order to assess the biological relevance of these patterns, we applied enrichment analyses for GO terms and "gene family conservation profiles" based on earlier annotations [16].

366

367 ***Sporozoites express genes which are evolutionarily unique to E. falciformis***

368 Sporozoites are in our study released from oocysts in vitro, after which they are capable of
 369 invading host cells. We suggest that the requirement for proteins which mediate motility and
 370 other invasion processes are reflected by their mRNA levels in the transcriptome. We find that
 371 *E. falciformis* sporozoites are defined by a group of genes (Ef-cluster 4, Figure 4B) that is
 372 largely specific to *E. falciformis* (Table 3). This indicates that *E. falciformis* does not share with
 373 other species many of the abundant sporozoite genes so far described for those Coccidia.
 374 Interestingly, five out of 12 SAG gene transcripts predicted for *E. falciformis* [16] are typical for
 375 sporozoites. SAG proteins are thought to be involved in host cell attachment and invasion, and
 376 possibly in induction of immune responses in other apicomplexan species [46,50,52–56]. In
 377 total, mRNAs encoding ten SAGs were detected as differentially abundant in our data, but in
 378 other lifecycle stages than sporozoites. Such expression of particular SAGs in stages other
 379 than sporozoites has been reported for *E. tenella* [57]. Genes also receiving attention as
 380 potential virulence factors in *E. tenella* are rhoptry kinases (RopKs) [58]. Transcripts of two out
 381 of ten *E. falciformis* orthologues of RopKs are highly abundant in sporozoites (Ef_cluster 4).
 382 Also in *E. tenella* some RopKs are expressed predominantly in sporozoites and have been
 383 shown to be differentially expressed compared to *E. tenella* intracellular merozoite stages [59].
 384 For genes with orthologues known to be important in other Coccidia, e.g., SAGs and RopKs,
 385 orthologues indicate a molecular function, but the biological relevance of their expression in *E.*
 386 *falciformis* remains unclear.

387

388 Genes typical for the sporozoite stage displayed a species specific profile with the respective
 389 gene families absent outside *E. falciformis* (Table 3). This mirrors our analysis of orthologous

390genes, in which sporozoites were the only lifecycle stage not displaying strong cross-species
391correlation in their transcriptome. This suggests that traits involved in host cell invasion may
392have evolved quickly and rapidly become specific for a parasite in its respective host species
393or target organ niche.

394

395For the overall biological functions of sporozoite genes (Ef-cluster 4), GO enrichment data
396suggests ATP production and biosynthesis processes as dominant features (Table S2). In
397addition, this invasive stage is characterized by "maintenance of protein location in cell" and
398GO terms which indicate similar biological functions. Possibly, this reflects control of
399microneme or rhoptry protein localization as sporozoites prepare for invasion. Sporozoites
400therefore display a transcriptome indicative of large requirements for ATP and production of
401known virulence factors such as SAG and RopKs and are characterized by expression of
402species specific genes.

403

404Genes typical for the sporozoite stage displayed a species specific profile with the respective
405gene families absent outside *E. falciformis* (Table 3). This mirrors our analysis of orthologous
406genes, in which sporozoites were the only lifecycle stage not displaying strong cross-species
407correlation in their transcriptome. This suggests that traits involved in host cell invasion may
408have evolved quickly and rapidly become specific for a parasite in its respective host species
409or target organ niche.

410

411***Growth processes dominate the transcriptome during asexual reproduction***

412 Invasion of epithelial cells by sporozoites is followed by asexual reproduction leading to a
413 massive increase in parasite numbers between 3 and 5 days post infection, when several
414 rounds of schizogony take place in a somewhat unsynchronized fashion [17,19]. In early
415 infection, and similar to sporozoites, mRNAs annotated for biosynthetic activity are enriched,
416 but different genes/mRNAs are contributing to enrichment of similar GO terms compared to
417 sporozoites (Table S2). Enrichment of terms referring to replication and growth-related
418 processes (biosynthesis) highlights the parasite's expansion during schizogony.

419
420 Amongst early infection high abundance mRNAs, we found four out of ten RopKs which are
421 predicted in *E. falciformis* [16]. This is the largest number of RopKs in any one group of
422 differentially abundant mRNAs in our analysis and they constitute a statistically significant
423 enrichment (Fisher's exact test; $p < 0.001$). Three of these have orthologues in *T. gondii*:
424 ROP41, ROP35 and ROP21 [60-63]. Our data gives a first overview of expression patterns for
425 *E. falciformis* RopKs and offer a good starting point for functional analysis of these virulence
426 factors in *Eimeria* spp..

427
428 ***Gametocyte motility dominates the transcriptome late in infection***
429 Two *E. falciformis* gene clusters show a distinct profile characterized by high mRNA
430 abundance on 7 days post infection (Ef-clusters 2 and 7; Figure 4B). Both clusters display low
431 mRNA abundance in other lifecycle stages, especially in oocysts and sporozoites. Enriched
432 GO terms such as "movement of cell or subcellular component" and "microtubule-based
433 movement" along with terms suggesting ATP production (e.g. "ATP generation from ADP")
434 indicate the presence of motile and energy demanding gametocytes in these samples. Peptide

435and nitrogen compound biosynthetic processes along with "chitin metabolic process" (Table
436S2) also suggest that the parasite produces building blocks for oocysts and their walls in this
437stage. Our data confirms findings of Walker et al. (2015) in *E. tenella* gametocytes: these
438authors also identified cytoskeleton related and transport processes as upregulated in
439gametocytes compared to merozoites or sporozoites [47].

440

441 **Oocysts are characterized by cell differentiation and DNA replication processes**

442Oocysts are the infective stage in the lifecycle of Coccidia. They are shed with feces as
443unsporulated, "immature", capsules and in the environment they undergo sporulation – meiotic
444and mitotic divisions [14] – and become infective. Our oocysts were purified in the
445unsporulated stage from passage in lab mice. Two expression clusters of mRNA are highly
446abundant in this stage (Ef-clusters 1 and 5; Figure 4B). One of these oocyst gene sets (Ef-
447cluster 5) is enriched for apicomplexan-shared orthologues (Table 3) and for GO terms such as
448"DNA repair", "protein modification process" and "cell differentiation", supporting that expected
449sporulation processes have been initiated. The same cluster is also the only cluster which is
450enriched for transmembrane domains (Fisher's exact test, FDR < 0.001).

451

452 ***E. falciformis* does not respond plastically to differences in the host transcriptome**

453We show that infections of *E. falciformis* in its natural host, the house mouse, follow a
454genetically canalized and chronological pattern independent of the immune status of the host.
455This is supported by the lack of separation of parasite transcriptomes from immune competent
456and immune deficient hosts, or from naïve and challenge infected hosts (Figure 4B). In the
457immune competent host, a switch from epithelial remodeling and innate immune processes to

adaptive immune responses between 5 and 7 days post infection are paralleled by a parasite switch from asexual to sexual reproduction. This contemporaneity might be an evolutionary adaptation of the parasite to host responses in order to finish its lifecycle before the host environment becomes hostile. Such a response could be based on a) genetically canalized developmental timing or b) the parasite sensing an immune challenge and establishing a reaction, i.e. respond plastically. However, in an immune deficient host, which lacks the described responses in its transcriptome, the parasite's transcriptome cannot be distinguished from one in an immune competent host. We thereby provide evidence from hosts with variation in their immune responses that support that *E. falciformis* follows a non-plastic, and instead genetically canalized program during its lifecycle in the mouse host.

Conclusion

In this dual transcriptome study, we provide a thorough description of transcriptional responses in mice to infection with *E. falciformis*, and corresponding parasite transcriptomes. The mouse epithelial transcriptome of naïve, immune competent mice changes upon infection. Responses in wild-type challenge infected hosts suggest strong regulation both at the transcriptional level and in RNA processing. In contrast, these patterns are missing in immunocompromised animals which instead show a minimal transcriptional response to infection, demonstrating the host dependence of mature T- and B-cells for a natural response to this coccidian parasite.

For the first time we also describe the full parasite lifecycle transcriptomes of *E. falciformis*. Parasite transcriptomes are not distinguishable between hosts of different immune competence, demonstrating lack of plasticity at the gene expression and mRNA levels. Two

independent assessments of evolutionary conservation show that invasive sporozoites possess the most species-specific transcriptomes in the *E. falciformis* lifecycle. We therefore suggest that excysted sporozoites express most of the genes involved in host-parasite co-evolutionary processes, which accelerate divergence and may determine niche specificity.

Taken together, we propose that *E. falciformis* follows a genetically predetermined path rather than responding to cues from the host, such as differences in immune responses. We further suggest that analyzing plasticity in parasites and comparing this between different host genotypes or species can be a useful tool to understand the evolutionary development of niche specificity or a generalist parasitic life-style infecting multiple different hosts or tissues. We emphasize that gene expression is not necessarily a product of plastic host-parasite interactions, especially not in the parasite, but may instead follow genetically determined programs.

METHODS

Mice, infection procedure and infection analysis

Three strains of mice were used in our experiments: NMRI, C57BL/6 (Charles River Laboratories, Sulzfeld, Germany), and *Rag1*^{-/-} on C57BL/6 background (obtained from German Rheumatism Research Centre, Berlin). *Rag1*^{-/-}-mice are deficient in T- and B-cell maturation. Animals were infected as described by Schmid et al. [64], but tap-water was used instead of PBS for administration of oocysts. Briefly, NMRI mice were infected two times, which will be referred to as naïve and challenge infection. For the naïve infection, 150 sporulated oocysts were administered in 100 µL water by oral gavage. During the naïve infection of 52 mice, all

504 animals were weighed every day. On day zero, before infection, as well as on 3 dpi, 5 dpi and
 505 7 dpi, ceca from 3-4 sacrificed mice per time-point were collected. Epithelial cells were isolated
 506 as described in Schmid et al. (2012), in which the protocol generated epithelial cells with 90 %
 507 purity. For challenge infection, mice recovered spontaneously and were after four weeks
 508 challenge infected. Recovery was monitored by weighing and visual inspection of fur. For the
 509 challenge infection, 1500 sporulated oocysts were applied by oral gavage in 100µL water (a
 510 higher dose was necessary to establish a challenge infection). Tissue from three to four mice
 511 per replicate was pooled for both non-reinfection control (referred to as day 0 of challenge
 512 infection) and for all other samples. *Rag1*^{-/-} mice and the background C57BL/6 strain control
 513 mice were also subjected to naïve and challenge infections with 10 sporulated oocysts in 100
 514 µL water in both cases. Samples were taken on day 0 (pre-infection control) and 5 dpi in both
 515 naïve and challenge infections of these mice and were otherwise treated as described above
 516 for NMRI mice. Oocyst shedding was determined from eight NMRI mice in naïve infection and
 517 four challenge infected, from 15 naïve *Rag1*^{-/-} and C57BL/6 mice respectively, and from nine
 518 challenge infected *Rag1*^{-/-} and C57BL/6 mice, respectively. Overall oocyst output was
 519 compared using Mann-Whitney U-test in R [65].

520

521 ***Oocyst purification for infection, sequencing and quantification***

522 Oocysts for infection were purified by NaOCl flotation of mouse feces stored in potassium
 523 dichromate, in which oocysts for infection were allowed to sporulate at room temperature for at
 524 least five days. During the patency phase, feces of mice were collected and oocysts were
 525 floated using saturated NaCl-solution. The oocyst output was quantified using the McMaster
 526 chamber. For sequencing, unsporulated oocysts were purified twice per day from feces of

527 NMRI mice on 8 – 10 dpi, and immediately subjected to RNA purification. The strain “*E.*
528 *falciformis* Bayer Haberkorn 1970” was used for all infections and parasite samples, it is
529 maintained through passage in NMRI mice in our facilities as described previously [64].

530

531 ***Sporozoite isolation***

532 Sporocysts were isolated according to the method of [66] with slight modifications. Briefly, not
533 more than 5 million sporulated oocysts were resuspended in 0.4% pepsin solution
534 (Applichem), pH 3, and incubated at 37°C for 1 hour. Subsequently, sporocysts were isolated
535 by mechanical shearing using glass beads (diameter 0.5 mm), washed and separated from
536 oocyst cell wall components by centrifugation at 1800 g for 10 min. Sporozoites were isolated
537 from sporocysts by in vitro excystation. For this, sporocysts were incubated at 37°C in DMEM
538 containing 0.04% tauroglycocholate (MP Biomedicals) and 0.25% trypsin (Applichem) for 30
539 min. Released sporozoites were purified in cellulose columns as described in [67].

540

541 ***RNA extraction and quantification***

542 For RNA-seq, total RNA was isolated either from infected epithelial cells, sporozoites, or
543 unsporulated oocysts using Trizol according to the manufacturer’s protocol (Invitrogen). In
544 addition, unsporulated oocysts in Trizol were treated by mechanical shearing using glass
545 beads for at least 20 min under frequent microscopic inspection. Purified RNA was used to
546 produce an mRNA library using Illumina’s TruSeq RNA Sample Preparation guide. For qPCR,
547 uninfected and infected epithelial cells from 3, 5 and 7 dpi were isolated as described above
548 and stored in 1 mL Trizol. Total RNA was isolated using the PureLink RNA Mini Kit (Invitrogen)

549and reverse transcribed into cDNA using the Superscript III Platinum Two Step qRT-PCR Kit
550(Thermo Fisher Scientific).

551These RNA preparations were used for RT-qPCR of *Eimeria* 18S and creation of a mouse
552gene reference index. For the reference index, the mouse genes cytochrome c-1 (Cyc),
553peptidylprolyl isomerase A (Ppia) and peptidylprolyl isomerase B (Ppib) were amplified using
554the primers Cyc1_qPCR_f (5'- CAGCTACCATGTCACAAGTAGC-3') and Cyc1_qPCR_r (5'-
555ACCACTTATGCCGCTTCATG -3'); Ppib_qPCR_f (CAAAGACACCAATGGCTCAC) and Ppib_
556qPCR_r (5'-TGACATCCTTCAGTGGCTTG-3'); Ppia_qPCR_f (5'-
557ACCGTGTTCCTTCGACATCAC-3') and Ppia_qPCR_r (5'-ATGGCGTGTAAGTCACCAC-3'),
558respectively. The *E. falciformis* 18S gene was amplified using the primers Ef18s_for (5'-
559ACAATTGGAGGGCAAGTCTG-3') and Ef18s_rev (5'-AAACACCAACAGACGCAGTG-3').

560After initialization at 50°C followed by activation of enzymes at 95°C, 40 amplification
561cycles consisting of denaturation at 95°C for 15s and combined annealing and elongation
562at 60°C for 60s were performed. After each cycle the fluorescent signal was measured. A
563reference index was constructed taking the cube root of the multiplied crossing threshold (ct)-
564values for the three mouse genes. This composite "index ct-value" was used to calculate the ct
565difference (delta-ct) of the *E. falciformis* 18S gene. The procedure was performed in technical
566triplicate for each sample and mean delta-ct values were taken. A linear model was
567constructed in R [65] to predict these normalized delta-ct values by day post infection (dpi) and
568type of infection (naïve or challenge infected). This model excludes measurements at 0 days
569post infection as background noise.

570

571

572 **Sequencing and quality assessment**

573 cDNA libraries were sequenced on either GAIIIX (13 samples) or Illumina Hiseq 2000 (14
574 samples) platforms in a total of four batches (different machine runs) as specified in Table 1. A
575 fastq_quality_filter (FASTQ-toolkit, version 0.0.14, available at
576 https://github.com/agordon/fastx_toolkit.git) was applied to Illumina Hiseq 2000 samples using
577 a phred score of 10. We intentionally did not use a stringent trimming before mapping to
578 genome assemblies as the mapping process itself has been shown to be a superior quality
579 control [68].

580

581 **Alignment and reference genomes**

582 The *Mus musculus* mm10 assembly (Genome Reference Consortium Mouse Build 38,
583 GCA_000001635.2) was used as reference genome for mapping and corresponding
584 annotations were used for downstream analyses. The *E. falciformis* genome [16] was
585 downloaded from ToxoDB [49]. For mapping, mouse and parasite genome files were merged
586 into a combined reference genome, and files including mRNA sequences from both species
587 were aligned against this reference using TopHat2, version 2.0.14, [69] with the option –G
588 specified, and Bowtie2, version 1.1.2, [70]. This was done to avoid spurious mapping in ultra-
589 conserved genomic regions. Single-end and pair-end sequence samples were aligned
590 separately with library type 'fr-unstranded' specified for pair-end samples. Bam files were used
591 as input for the function “featureCounts” from of the R package “Rsubread” [71]. All
592 subsequent analyses were performed in R [65].

593

594

595 **Differential mRNA abundance, data normalization and sample exclusions**

596 After import of data to R, mouse and parasite data was separated using transcript IDs and
 597 analyzed, including normalization, separately. For each species, count data was normalized
 598 using the R-package edgeR version 3.16.2 [72] with the upperquartile normalization method.
 599 This raw data underlying our study is available as supplementary data S1. Briefly, genes with
 600 below an overall of 3000 reads (mouse) and 100 reads (*E. falciformis*) summed over all
 601 samples (libraries) were removed and normalization factors were calculated for the 75%
 602 quantile for each library. This normalization is suitable for densities of mapping read counts
 603 which follow a negative binomial distribution. Technically, this exclusion made it possible to
 604 obtain parasite read counts in agreement with a negative binomial distribution. We excluded
 605 samples NMRI_2nd_3dpi_rep1 and NMRI_2nd_5dpi_rep2 due to low parasite contribution
 606 (0.012% and 0.023%) to the overall transcriptome. Technically, this exclusion made it possible
 607 to obtain parasite read counts in agreement with a negative binomial distribution. Both
 608 excluded samples are from challenge infection and it is likely that the infected mice were
 609 immune to re-infection. One additional sample (NMRI_1stInf_0dpi_rep1) was excluded
 610 because the uninfected control showed unexpected mapping of reads to the *E. falciformis*
 611 genome (0.033%). As samples and individual replicates were sequenced in batches to
 612 different depth and using different instrumentation (Table 1) we performed multidimensional
 613 scaling of samples as quality controls using the function “plotMDS” provided in the R package
 614 edgeR v 3.16.2 [72].

615

616

617

618 **Testing of differentially abundant mRNAs and hierarchical clustering**

619 We used edgeR v 3.16.2 [72] further to fit generalized linear models (GLMs with a negative
620 binomial link function) for each gene (glmFit) and to perform likelihood ratio tests for models
621 with or without a focal factor (glmLRT) using the “alternate design matrix” approach specifying
622 focal contrasts individually. Tested contrasts comprised for the mouse a) infections at each
623 time-point versus uninfected controls, b) corresponding time-points between different mouse
624 strains and c) corresponding time-points and mouse strains for naïve and challenge infection.
625 Since the control sample for infection in naïve NMRI mice was removed from the analysis (see
626 above), the two uninfected replicates from challenge infection were used as uninfected
627 controls in all NMRI mouse analyses. For the parasite, contrasts were set between a) all
628 different stages of the lifecycle, as well as b) and c) as above (see also results in Table 2).

629
630 Mouse mRNAs which responded to infection or were differently abundant at different time-
631 points of infection (0 vs “any days post infection” or “any days post infection” vs “any days post
632 infection”; see Table 2) and *E. falciformis* genes showing differences between any lifecycle
633 stage (oocysts versus sporozoites, or either of those versus “any days post infection” or “any
634 days post infection” versus “any days post infection”) were selected and used for hierarchical
635 clustering. Hierarchical clustering was performed using the complete linkage method based on
636 Euclidean distances between Z-scores (mRNA abundance values scaled for differences from
637 mean over all samples of each gene in units of standard deviations).

638

639

640

641 **Enrichment tests and evolutionary conservation test**

642 Gene Ontology (GO) enrichment analysis was performed using the R package topGO with the
 643 “weight01” algorithm and Fisher's exact tests. We additionally performed a correction for
 644 multiple testing on the returned p-values (function “p.adjust” using the BH-method [73]).
 645 Similarly, a Fisher's exact test and corrections for multiple testing were used to test for
 646 overrepresentation of transcripts with a signal sequence for entering the secretory pathway or
 647 containing transmembrane domains (as inferred using Signal P) which are predicted for the *E.*
 648 *falciformis* genome [16]. Evolutionary conservation of gene families was analyzed based on
 649 categories from [16] which are as follows: i) *E. falciformis* specific, ii) specific to the genus
 650 *Eimeria*, compiled by an analysis of *E. falciformis*, *E. maxima* and *E. tenella*, iii) Coccidia:
 651 *Eimeria* plus *T. gondii* and *Neospora caninum*, iv) Coccidia plus *Babesia microti*, *Theileria*
 652 *annulata*, *Plasmodium falciparum* and *Plasmodium vivax* v) the same apicomplexan parasites
 653 as in iv plus *Cryptosporidium hominis*, vi) universally conserved in the eukaryote super-
 654 kingdom inferred from an analysis of *Saccharomyces cerevisiae* and *Arabidopsis thaliana*.
 655 These categories were tested for overrepresentation in parasite gene clusters with particular
 656 patterns described in the text using Fisher's exact-tests. Resulting p-values were corrected for
 657 multiple testing using the procedure of Benjamini and Hochberg [72] and reported as false
 658 discovery rates (FDR).

659

660 **Correlation analysis of apicomplexan transcriptomes**

661 Transcriptome datasets from [46,47] and [48] were downloaded from ToxoDB [49].
 662 Orthologues between *E. falciformis*, *E. tenella* and *T. gondii* were compiled as in [16] and only
 663 1:1:1 orthologue triplets were retained for analysis, as multi-paralog gene-families might

664contain members showing divergent evolution of gene-expression due to neo/sub
665functionalization. Mean mRNA abundances per lifecycle stage were used for samples from our
666study. Spearman's correlation coefficients for expression over different samples in all studies
667and over different species represented by their orthologues were determined. Hierarchical
668clustering with complete linkage was used to cluster resulting correlations coefficients.

669

670

671**DECLARATIONS**

672

673***Ethics approval and consent to participate***

674Animal procedures were performed according to the German Animal Protection Laws as
675directed and approved by the overseeing authority Landesamt fuer Gesundheit und Soziales
676(Berlin, Germany) under numbers H0098/04 and G0039/11.

677

678***Consent to publish***

679Not applicable

680

681***Availability of data and materials***

682Raw data will be deposited to ENA/SRA. A processed version of this data will be available at
683ToxoDB (<http://toxodb.org/toxo/>) for interactive analysis and download. Code underlying our
684analysis and intermediate result files are available at https://github.com/derele/Ef_RNAseq
685tagged as version 0.1. And will be deposited upon acceptance in it's final version at Zenodo
686(<https://zenodo.org/>).

687

688 ***Competing interests***

689 The authors declare that they have no competing interests.

690

691 ***Funding***

692 The study was funded by the DFG Research Training Group 2046 "Parasite Infections: From
693 Experimental Models to Natural Systems" (TE) and DFG individual grant 285969495 (EH).

694

695 ***Authors' contributions***

696 TE, SS, CD, RL and EH designed the experiments, RL performed infections, EH obtained
697 grant support for the work, RL, SS, CD and EH gathered the data, EH and TE analyzed the
698 data, TE and EH drafted the manuscript, TE, SS, RL and EH edited the manuscript, all authors
699 contributed original ideas to the research and agreed on the final version of the manuscript.

700

701 ***Acknowledgements***

702 The authors wish to thank Frank Seeber and Toni Aebischer for valuable comments on the
703 manuscript, Annica Rebbig for establishing the mouse reference index for RT-qPCR and Kirsi
704 Blank for support in oocyst purification and counting, parasite passaging and RT-qPCRs.

705

706

707

708

709

710 Tables

711 **Table 1** Summary of data per sample, sorted according to number of reads mapping to the *E.*

712 *falciformis* genome.

Sample*	Sequencing method	Batch **	Total reads	Reads mapping mouse	Reads mapping <i>E. falciformis</i>	Percentage <i>E. falciformis</i>	# <i>E. falciformis</i> genes ****
NMRI_2ndInf_0dpi_rep1	GAI	2	108,937,797	70,489,674	247	0.0004	1
Rag_1stInf_0dpi_rep1	hiseq	3	25,362,793	18,853,850	443	0.0023	2
C57BL/6_1stInf_0dpi_rep1	hiseq	3	35,731,249	25,119,348	457	0.0018	2
C57BL/6_1stInf_0dpi_rep2	hiseq	3	47,085,959	34,377,133	608	0.0018	2
Rag_1stInf_0dpi_rep2	hiseq	3	46,556,156	35,233,327	676	0.0019	2
NMRI_2ndInf_0dpi_rep2	hiseq	3	58,122,244	40,794,245	3,406	0.0083	51
NMRI_2ndInf_3dpi_rep1****	hiseq	3	57,934,016	40,544,287	4,803	0.0118	95
NMRI_2ndInf_5dpi_rep2 ***	hiseq	3	63,965,539	48,289,181	10,941	0.0227	407
NMRI_1stInf_0dpi_rep1 ***	GAI	1	82,364,585	55,176,243	17,954	0.0325	701
NMRI_2ndInf_3dpi_rep2	hiseq	3	65,548,826	46,171,909	29,548	0.0640	1,580
NMRI_2ndInf_7dpi_rep2	hiseq	3	67,487,466	51,722,265	40,091	0.0775	1,836
Rag_1stInf_5dpi_rep1	hiseq	3	38,651,359	29,982,453	63,024	0.2098	2,548
Rag_1stInf_5dpi_rep2	hiseq	3	34,779,832	25,297,803	99,000	0.3898	2,828
C57BL/6_1stInf_5dpi_rep1	hiseq	3	40,904,388	29,319,604	185,969	0.6303	4,173
Rag_2ndInf_5dpi_rep1	hiseq	3	50,049,848	37,093,621	192,856	0.5172	4,167
C57BL/6_1stInf_5dpi_rep2	hiseq	3	29,511,368	18,062,349	215,696	1.1801	3,823
C57BL/6_2ndInf_5dpi_rep1	hiseq	3	35,148,432	25,660,184	262,909	1.0142	4,563
NMRI_1stInf_3dpi_rep1	GAI	1	73,236,430	49,993,358	394,384	0.7827	5,220
NMRI_1stInf_3dpi_rep2	GAI	2	160,709,694	117,791,044	413,051	0.3494	4,862
NMRI_1stInf_5dpi_rep2	GAI	2	119,902,722	76,419,774	794,570	1.0290	5,333
NMRI_2ndInf_5dpi_rep1	GAI	2	230,773,955	143,186,486	1,846,840	1.2734	5,533
NMRI_2ndInf_7dpi_rep1	hiseq	3	70,366,762	41,467,146	3,634,201	17.2335	5,875
NMRI_1stInf_5dpi_rep1	GAI	2	76,702,168	47,037,087	3,669,701	15.5631	5,700
Sporozoites_rep2	GAI	0	19,551,681	3,656	11,470,604	99.9246	5,513
NMRI_1stInf_5dpi_rep3	GAI	0	191,099,180	33,735,624	27,839,458	24.9513	5,784
NMRI_1stInf_7dpi_rep1	GAI	1	66,505,514	3,310,666	39,400,884	92.2488	5,932
Sporozoites_rep1	GAI	1	67,325,397	4,334	43,774,401	99.9901	5,825
Oocysts_rep1	GAI	1	68,859,802	3,805	49,653,065	99.9923	5,695
Oocysts_rep2	GAI	0	151,090,783	18,524	71,019,860	99.9739	5,777
NMRI_1stInf_7dpi_rep2	GAI	1	139,749,046	21,699,324	73,539,445	77.2159	5,943

713

714* Sample names are given with information separated by underscore as follows: 1) mouse
715strain, 2) naïve (1st) or challenge (2nd) infection, 3) dpi (days post infection), and 4) replicate
716number.

717** Number of expressed *E. falciformis* genes (read counts >5).

718*** These samples were removed from downstream analyses because of uncertain infection
719status.

720

721**Table 2** Number of mouse and *E. falciformis* mRNAs significantly differentially abundant in
722different comparisons (Contrasts). Empty cells indicate that comparison is not applicable.

Contrast	Number of <i>E. falciformis</i> mRNAs with FDR < 0.01	Number of mouse mRNAs with FDR < 0.01
NMRI 7 dpi vs. uninfected control		2,711
NMRI 5 dpi vs. uninfected control		1,804
NMRI 3 dpi vs. NMRI 7 dpi	1,399	1,322
C57BL/6 5 dpi vs. uninfected control		919
NMRI 7 dpi naïve vs NMRI 7 dpi challenge	0	857
NMRI 5 dpi vs. NMRI 7 dpi	2,084	732
<i>Rag1</i> ^{-/-} vs C57BL/6		362
NMRI 3 dpi vs ctrl		325
C57BL/6 5 dpi naïve vs C57BL/6 5 dpi challenge	0	175
<i>Rag1</i> ^{-/-} 5 dpi vs control		42
NMRI 3 dpi naïve vs NMRI 3 challenge	1	18
NMRI 3 dpi vs. NMRI 5 dpi	103	0
NMRI 5 dpi vs. oocysts	3,691	
Sporozoites vs. oocysts	3,532	
NMRI 3 dpi vs. oocysts	3,303	
NMRI 7 dpi vs. oocysts	3,202	
NMRI 7 dpi vs. sporozoites	2,663	
NMRI 5 dpi vs. sporozoites	1,726	
NMRI 3 dpi vs. sporozoites	1,705	
NMRI control vs. C57BL/6 control	13	

723

Table 3 Enrichments and underrepresentation of species or species-group orthologues in *E. falciformis* gene clusters (from Figure 3b). Odds ratios higher than one indicate enrichment and smaller than one indicate underrepresentation. Conservation categories were chosen as previously described [16]. Only significant results (FDR < 0.05) are shown.

<i>E. falciformis</i> cluster	Conservation category	Odds ratio	p-value	FDR
Ef-cluster 2 (up at 7 dpi)	Conserved	0.67	9.03E-06	1.90E-04
Ef-cluster 4 (up in sporozoites)	Conserved	0.72	2.44E-04	1.71E-03
Ef-cluster 7 (up at 7 dpi)	Conserved	1.72	1.11E-10	4.65E-09
Ef-cluster 2 (up at 7 dpi)	ApicomplexaC	0.45	1.84E-04	1.71E-03
Ef-cluster 5 (up in oocysts)	ApicomplexaC	1.86	3.76E-05	5.26E-04
Ef-cluster 4 (up in sporozoites)	<i>E. falciformis</i>	3.05	2.38E-04	1.71E-03
Ef-cluster 1 (up in oocysts)	<i>Eimeria</i>	0.68	1.83E-03	9.59E-03
Ef-cluster 6 (up in early inf)	Apicomplexa	1.46	1.11E-03	6.64E-03

728

729

730 Figures

Figure 1. Oocyst output and changes in intensity of *E. falciformis* infection in mouse. Oocyst counts in naïve and challenge infection are shown for three different mouse strains. For infection of naïve NMRI 150 oocysts were used, for challenge infection 1500 oocysts. For C57BL/6 and *Rag1*^{-/-} mice 10 oocysts were used in each infection. A) Overall output of shed oocysts and B) shedding kinetics are depicted. C) RT-qPCR data of *E. falciformis* 18S in NMRI mice displays an increase in parasite mRNA over the course of infection. Significantly less parasite 18S transcripts (normalized against host transcripts of house-keeping genes) were detected in challenge infected mice. Formulas and prediction lines are given for linear models. D) The percentage of parasite mRNA detected by RNA-seq increases during infection (shown for NMRI). More mRNA is detected in naïve mice compared to challenge infected mice. Sporozoites and oocysts contained ~100% parasite material.

742

743 **Figure 2.** Differentially abundant mouse mRNAs and clustering thereof. A) Venn diagram
 744 visualizes the overlap between genes showing differential abundance (FDR < 0.01; edgeR glm
 745 likelihood-ratio tests) between i) uninfected controls and different time-points post infection and
 746 ii) between different time-points and the sum of all genes reacting to infection. Controls from
 747 challenge infection were used. B) Hierarchical clustering of differentially abundant mRNAs
 748 performed on Euclidean distances using complete linkage. Cluster cut-offs (dendrogram
 749 resolution) were set to identify gene-sets with profiles interpretable in relation to the parasite
 750 lifecycle and between mice of different immune competence.

751

752 **Figure 3.** Correlations of *E. falciformis* mRNA abundance with orthologues from other Coccidia.
 753 *E. falciformis* mRNA abundance was compared to that of orthologous genes of *E. tenella*
 754 [46,47] and *T. gondii* [48]. Correlation coefficients (Spearman's ρ) were clustered using
 755 complete linkage. *T. gondii* and *Eimeria* spp. “late infection” samples cluster together. *E.*
 756 *falciformis* early infection samples cluster with *E. tenella* merozoites. *E. falciformis* sporozoites
 757 cluster with *E. falciformis* early infection, whereas unsporulated oocysts cluster with *E. tenella*
 758 unsporulated oocysts.

759

760 **Figure 4.** Differentially abundant *E. falciformis* mRNAs and clustering thereof. A) Venn diagram
 761 visualizes the overlap between genes showing differential abundance (FDR < 0.01; edgeR glm
 762 likelihood-ratio tests) between intracellular stages at 3 days post infection, 5 days post
 763 infection and 7 days post infection. B) Hierarchical clustering of abundance profiles for
 764 differentially abundant mRNAs performed on Euclidean distances using complete linkage.

765 Cluster cut-offs (dendrogram resolution) were set to identify gene-sets with profiles
766 interpretable in relation to the parasite lifecycle.

767

768 SUPPLEMENTARY INFORMATION

769

770 Supplementary Figures

771 **Figure S1.** Ordinations on mouse and parasite transcriptomes. The results of multidimensional
772 scaling analyses are displayed for mouse and *E. falciformis* using different labels to allow
773 comparisons.

774 **Figure S2.** Controls for the properties of mRNA abundance distributions after setting different
775 abundance thresholds per mRNA over all samples.

776 **Figure S3.** Mouse mRNA abundance in late *E. falciformis* infection versus uninfected controls,
777 assessed by both RNA-seq (present data) and microarray. Mouse data from 7 days post
778 infection (RNA-seq) and 6 days post infection. In both experiments, NMRI mice were infected
779 with the same *E. falciformis* isolate. Even with one day difference in sampling, mouse
780 transcriptomes show a strong correlation. The line depicted for visualisation corresponds to
781 generalized additive model using penalized regression splines.

782 **Figure S4.** Weight loss of mice during *E. falciformis* infection.

783 Mouse weight is shown as a percentage relative to weight at the time of infection. Infection
784 dose for NMRI was 150 oocysts in naïve infection and 1500 in challenge infection. For
785 C57BL/6 and Rag1^{-/-} dose was 10 oocysts in both naïve and challenge infection. Bars indicate
786 standard error for three or four replicates.

787

788 **Supplementary Tables**

789 Table S1: GO terms enriched in Mm-clusters in Figure 2B.

790 Table S2: GO terms enriched in Ef-clusters in Figure 4B.

791

792 **REFERENCES**

793

1. Stearns SC. The evolutionary significance of phenotypic plasticity. *BioScience*. 1989;39:436–45.
2. Dodson S. Predator-induced reaction norms. *BioScience*. 1989;39:447–52.
3. Pancer Z, Cooper MD. The evolution of adaptive immunity. *Annu. Rev. Immunol.* 2006;24:497–518.
4. Viney M, Diaz A. Phenotypic plasticity in nematodes. *Worm*. 2012;1:98–106.
5. Stear MJ, Bairden K, Duncan JL, Holmes PH, McKellar QA, Park M, et al. How hosts control worms. *Nature*. 1997;389:27–27.
6. Weclawski U, Heitlinger EG, Baust T, Klar B, Petney T, Han Y-S, et al. Rapid evolution of *Anguillicola crassus* in Europe: species diagnostic traits are plastic and evolutionarily labile. *Front. Zool.* 2014;11:74.
7. Weclawski U, Heitlinger EG, Baust T, Klar B, Petney T, San Han Y, et al. Evolutionary divergence of the swim bladder nematode *Anguillicola crassus* after colonization of a novel host, *Anguilla anguilla*. *BMC Evol. Biol.* 2013;13:78.
8. Heitlinger E, Taraschewski H, Weclawski U, Gharbi K, Blaxter M. Transcriptome analyses of *Anguillicola crassus* from native and novel hosts. *PeerJ*. 2014;2:e684.
9. Weber C, Koutero M, Dillies M-A, Varet H, Lopez-Camarillo C, Coppée JY, et al. Extensive transcriptome analysis correlates the plasticity of *Entamoeba histolytica* pathogenesis to rapid phenotype changes depending on the environment. *Sci. Rep.* 2016. <http://www.ncbi.nlm.nih.gov/pmc/articles/PMC5073345/>. Accessed 23 Feb 2017.
10. Lovegrove FE, Peña-Castillo L, Mohammad N, Liles WC, Hughes TR, Kain KC. Simultaneous host and parasite

expression profiling identifies tissue-specific transcriptional programs associated with susceptibility or resistance to experimental cerebral malaria. *BMC Genomics*. 2006;7:295.

11. da Silva F, da Fonseca M, Barbosa HS, Gross U, Lüder CGK. Stress-related and spontaneous stage differentiation of *Toxoplasma gondii*. *Mol. Biosyst.* 2008;4:824–34.

12. Buchholz KR, Fritz HM, Chen X, Durbin-Johnson B, Rocke DM, Ferguson DJ, et al. Identification of tissue cyst wall components by transcriptome analysis of in vivo and in vitro *Toxoplasma gondii* bradyzoites. *Eukaryot. Cell.* 2011;10:1637

13. Sibley DL, Charron A, Håkansson S, Mordue D. Invasion and Intracellular Survival by *Toxoplasma*. In: *Madame Curie Bioscience Database [Internet]*. Austin (TX): Landes Bioscience; 2000-2013. Available from: <https://www.ncbi.nlm.nih.gov/books/NBK6450/2013>

14. Duszynski DW. *Eimeria*, *Eimeria*. eLS. John Wiley & Sons, Ltd. 2011.

<http://onlinelibrary.wiley.com/doi/10.1002/9780470015902.a0001962.pub2/abstract>. Accessed 10 Oct 2016.

15. Chapman HD, Barta JR, Blake D, Gruber A, Jenkins M, Smith NC, et al. A selective review of advances in coccidiosis research. *Adv. Parasitol.* 2013;83:93.

16. Heitlinger E, Spork S, Lucius R, Dieterich C. The genome of *Eimeria falciformis* - reduction and specialization in a single host apicomplexan parasite. *BMC Genomics*. 2014;15:696.

17. Haberkorn A. Die Entwicklung von *Eimeria falciformis* (Eimer 1870) in der weißen Maus (*Mus musculus*). *Z. Für Parasitenkd.* 1970;34:49–67.

18. Schmid M, Heitlinger E, Spork S, Mollenkopf H-J, Lucius R, Gupta N. *Eimeria falciformis* infection of the mouse cecum identifies opposing roles of IFN γ -regulated host pathways for the parasite development. *Mucosal Immunol.* 2013;7:969-982

19. Mesfin GM, Bellamy JEC. Effects of acquired resistance on infection with *Eimeria falciformis* var. *pragensis* in mice. *Infect. Immun.* 1979;23:108–14.

20. Montes C, Rojo F, Hidalgo R, Ferre I, Badiola C. Selection and development of a Spanish precocious strain of *Eimeria necatrix*. *Vet. Parasitol.* 1998;78:169–83.

21. Pakandl M. Selection of a precocious line of the rabbit coccidium *Eimeria flavescens* Marotel and Guilhon (1941) and characterisation of its endogenous cycle. *Parasitol. Res.* 2005;97:150–5.
22. Rose ME. Immune responses in infections with Coccidia: Macrophage activity. *Infect. Immun.* 1974;10:862–71.
23. Blagburn BL, Todd KS. Pathological changes and immunity associated with experimental *Eimeria vermiformis* infections in *Mus musculus*. *J. Protozool.* 1984;31:556–61.
24. Rose ME, Hesketh P, Wakelin D. Immune control of murine coccidiosis: CD4⁺ and CD8⁺ T lymphocytes contribute differentially in resistance to primary and secondary infections. *Parasitology.* 1992;105:349–54.
25. Gadde U, Chapman HD, Rathinam TR, Erf GF. Acquisition of immunity to the protozoan parasite *Eimeria adenoeides* in turkey poults and the peripheral blood leukocyte response to a primary infection. *Poult. Sci.* 2009;88:2346–52.
26. Sühwold A, Hermosilla C, Seeger T, Zahner H, Taubert A. T-cell reactions of *Eimeria bovis* primary- and challenge-infected calves. *Parasitol. Res.* 2010;106:595–605.
27. Stange J, Hepworth MR, Rausch S, Zajic L, Kühl AA, Uyttenhove C, et al. IL-22 mediates host defense against an intestinal intracellular parasite in the absence of IFN- γ at the cost of Th17-driven immunopathology. *J. Immunol. Baltim. Md* 1950. 2012;188:2410–8.
28. Foth BJ, Zhang N, Chahal BK, Sze SK, Preiser PR, Bozdech Z. Quantitative time-course profiling of parasite and host cell proteins in the human malaria parasite *Plasmodium falciparum*. *Mol. Cell. Proteomics MCP.* 2011;10:1-16.
29. Li Y, Shah-Simpson S, Okrah K, Belew AT, Choi J, Caradonna KL, et al. Transcriptome remodeling in *Trypanosoma cruzi* and human cells during intracellular infection. *PloS Pathog.* 2016;12:e1005511.
30. Fernandes MC, Dillon LAL, Belew AT, Bravo HC, Mosser DM, El-Sayed NM. Dual transcriptome profiling of *Leishmania*-infected human macrophages reveals distinct reprogramming signatures. *mBio.* 2016;7:e00027-16.
31. Westermann AJ, Förstner KU, Amman F, Barquist L, Chao Y, Schulte LN, et al. Dual RNA-seq unveils noncoding RNA functions in host-pathogen interactions. *Nature.* 2016;529:496–501.

32. Rosani U, Varotto L, Domeneghetti S, Arcangeli G, Pallavicini A, Venier P. Dual analysis of host and pathogen transcriptomes in ostreid herpesvirus 1-positive *Crassostrea gigas*. *Environ. Microbiol.* 2015;17:4200–12.
33. Ovington KS, Alleva LM, Kerr EA. Cytokines and immunological control of *Eimeria* spp. *Int. J. Parasitol.* 1995;25:1331–51.
34. Stephenson LS, Latham MC, Ottesen EA. Malnutrition and parasitic helminth infections. *Parasitology.* 2000;121:S23–38.
35. Aloisio F, Filippini G, Antenucci P, Lepri E, Pezzotti G, Cacciò SM, et al. Severe weight loss in lambs infected with *Giardia duodenalis* assemblage B. *Vet. Parasitol.* 2006;142:154–8.
36. Preston-Mafham RA, Sykes AH. Changes in body weight and intestinal absorption during infections with *Eimeria acervulina* in the chicken. *Parasitology.* 1970;61:417.
37. Sharman PA, Smith NC, Wallach MG, Katrib M. Chasing the golden egg: Vaccination against poultry coccidiosis. *Parasite Immunol.* 2010;32:590-98
38. Stange J. Studies on host-pathogen interactions at mucosal barrier surfaces using the murine intestinal parasite *Eimeria falciformis* - Deutsche Digitale Bibliothek. 2012. <http://www.deutsche-digitale-bibliothek.de/item/DDAKP5LJSJBAPPALDVQ5Y52YV3AG7NCL>. Accessed 16 Dec 2016
39. Kuhn KA, Manieri NA, Liu T-C, Stappenbeck TS. IL-6 stimulates intestinal epithelial proliferation and repair after injury. *PloS One.* 2014;9:e114195.
40. Park H, Li Z, Yang XO, Chang SH, Nurieva R, Wang Y-H, et al. A distinct lineage of CD4 T-cells regulates tissue inflammation by producing interleukin 17. *Nat. Immunol.* 2005;6:1133–41.
41. Beck PL, Rosenberg IM, Xavier RJ, Koh T, Wong JF, Podolsky DK. Transforming growth factor-beta mediates intestinal healing and susceptibility to injury in vitro and in vivo through epithelial cells. *Am. J. Pathol.* 2003;162:597–608.
42. Suzuki A, Sekiya S, Gunshima E, Fujii S, Taniguchi H. EGF signaling activates proliferation and blocks apoptosis of mouse and human intestinal stem/progenitor cells in long-term monolayer cell culture. *Lab. Investig. J. Tech. Methods Pathol.* 2010;90:1425–36.

43. Kaiser GC, Polk DB. Tumor necrosis factor alpha regulates proliferation in a mouse intestinal cell line. *Gastroenterology*. 1997;112:1231–40.
44. VanDussen KL, Carulli AJ, Keeley TM, Patel SR, Puthoff BJ, Magness ST, et al. Notch signaling modulates proliferation and differentiation of intestinal crypt base columnar stem cells. *Dev. Camb. Engl.* 2012;139:488–97.
45. Macian F. NFAT proteins: key regulators of T-cell development and function. *Nat. Rev. Immunol.* 2005;5:472–84.
46. Reid AJ, Blake DP, Ansari HR, Billington K, Browne HP, Bryant JM, et al. Genomic analysis of the causative agents of coccidiosis in domestic chickens. *Genome Res.* 2014;gr.168955.113–.
47. Walker R a, Sharman P a, Miller CM, Lippuner C, Okoniewski M, Eichenberger RM, et al. RNA Seq analysis of the *Eimeria tenella* gametocyte transcriptome reveals clues about the molecular basis for sexual reproduction and oocyst biogenesis. *BMC Genomics.* 2015;16:1–20.
48. Hehl AB, Basso WU, Lippuner C, Ramakrishnan C, Okoniewski M, Walker RA, et al. Asexual expansion of *Toxoplasma gondii* merozoites is distinct from tachyzoites and entails expression of non-overlapping gene families to attach, invade, and replicate within feline enterocytes. *BMC Genomics.* 2015;16:66.
49. Gajria B, Bahl A, Brestelli J, Dommer J, Fischer S, Gao X, et al. ToxoDB: an integrated *Toxoplasma gondii* database resource. *Nucleic Acids Res.* 2007;36:D553–6.
50. Reid AJ, Vermont SJ, Cotton JA, Harris D, Hill-Cawthorne GA, Könen-Waisman S, et al. Comparative genomics of the Apicomplexan parasites *Toxoplasma gondii* and *Neospora caninum*: Coccidia differing in host range and transmission strategy. *PLoS Pathog.* 2012;8:e1002567.
51. Gardner MJ, Hall N, Fung E, White O, Berriman M, Hyman RW, et al. Genome sequence of the human malaria parasite *Plasmodium falciparum*. *Nature.* 2002;419:498–511.
52. Mineo JR, Kasper LH. Attachment of *Toxoplasma gondii* to host cells involves major surface protein, SAG-1 (P-30). *Exp. Parasitol.* 1994;79:11–20.
53. Grimwood J, Smith JE. *Toxoplasma gondii*: the role of parasite surface and secreted proteins in host cell invasion. *Int. J.*

Parasitol. 1996;26:169–73.

54. Cowman AF, Crabb BS. Invasion of red blood cells by malaria parasites. *Cell*. 2006;124:755–66.

55. Carruthers V, Boothroyd JC. Pulling together: an integrated model of *Toxoplasma* cell invasion. *Curr. Opin. Microbiol.* 2007;10:83–9.

56. Chow Y-P, Wan K-L, Blake DP, Tomley F, Nathan S. Immunogenic *Eimeria tenella* glycosylphosphatidylinositol-anchored surface antigens (SAGs) induce inflammatory responses in avian macrophages. *PLoS ONE*. 2011
<http://www.ncbi.nlm.nih.gov/pmc/articles/PMC3182191/>. Accessed 29 Dec 2016.

57. Tabarés E, Ferguson D, Clark J, Soon P-E, Wan K-L, Tomley F. *Eimeria tenella* sporozoites and merozoites differentially express glycosylphosphatidylinositol-anchored variant surface proteins. *Mol. Biochem. Parasitol.* 2004;135:123–32.

58. Talevich E, Kannan N. Structural and evolutionary adaptation of rhoptry kinases and pseudokinases, a family of coccidian virulence factors. *BMC Evol. Biol.* 2013;13:117.

59. Oakes RD, Kurian D, Bromley E, Ward C, Lal K, Blake DP, et al. The rhoptry proteome of *Eimeria tenella* sporozoites. *Int. J. Parasitol.* 2013;43:181–8.

60. Taylor S, Barragan A, Su C, Fux B, Fentress SJ, Tang K, et al. A secreted serine-threonine kinase determines virulence in the eukaryotic pathogen *Toxoplasma gondii*. *Science*. 2006;314:1776–80.

61. Saeij JPJ, Collier S, Boyle JP, Jerome ME, White MW, Boothroyd JC. *Toxoplasma* co-opts host gene expression by injection of a polymorphic kinase homologue. *Nature*. 2007;445:324–7.

62. Fleckenstein MC, Reese ML, Könen-Waisman S, Boothroyd JC, Howard JC, Steinfeldt T. A *Toxoplasma gondii* Pseudokinase Inhibits Host IRG Resistance Proteins. *PloS Biol.* 2012;10:e1001358.

63. Fox BA, Rommereim LM, Guevara RB, Falla A, Triana MAH, Sun Y, et al. The *Toxoplasma gondii* rhoptry kinome is essential for chronic infection. *mBio*. 2016;7:e00193-16.

64. Schmid M, Lehmann MJ, Lucius R, Gupta N. Apicomplexan parasite, *Eimeria falciformis*, co-opts host tryptophan

catabolism for life cycle progression in mouse. *J. Biol. Chem.* 2012;287:20197–20207.

65. R Development Core Team. R: A language and environment for statistical computing. R Foundation for Statistical Computing, Vienna, Austria. 2008. <http://www.R-project.org>

66. Kowalik S, Zahner H. *Eimeria separata*: method for the excystation of sporozoites. *Parasitol. Res.* 1999;85:496–9.

67. Schmatz DM, Crane MSJ, Murray PK. Purification of *Eimeria* sporozoites by DE-52 anion exchange chromatography. *J. Protozool.* 1984;31:181–183.

68. MacManes MD. On the optimal trimming of high-throughput mRNA sequence data. *Front. Genet.* 2014. <http://journal.frontiersin.org/article/10.3389/fgene.2014.00013/abstract>. Accessed 29 Dec 2016.

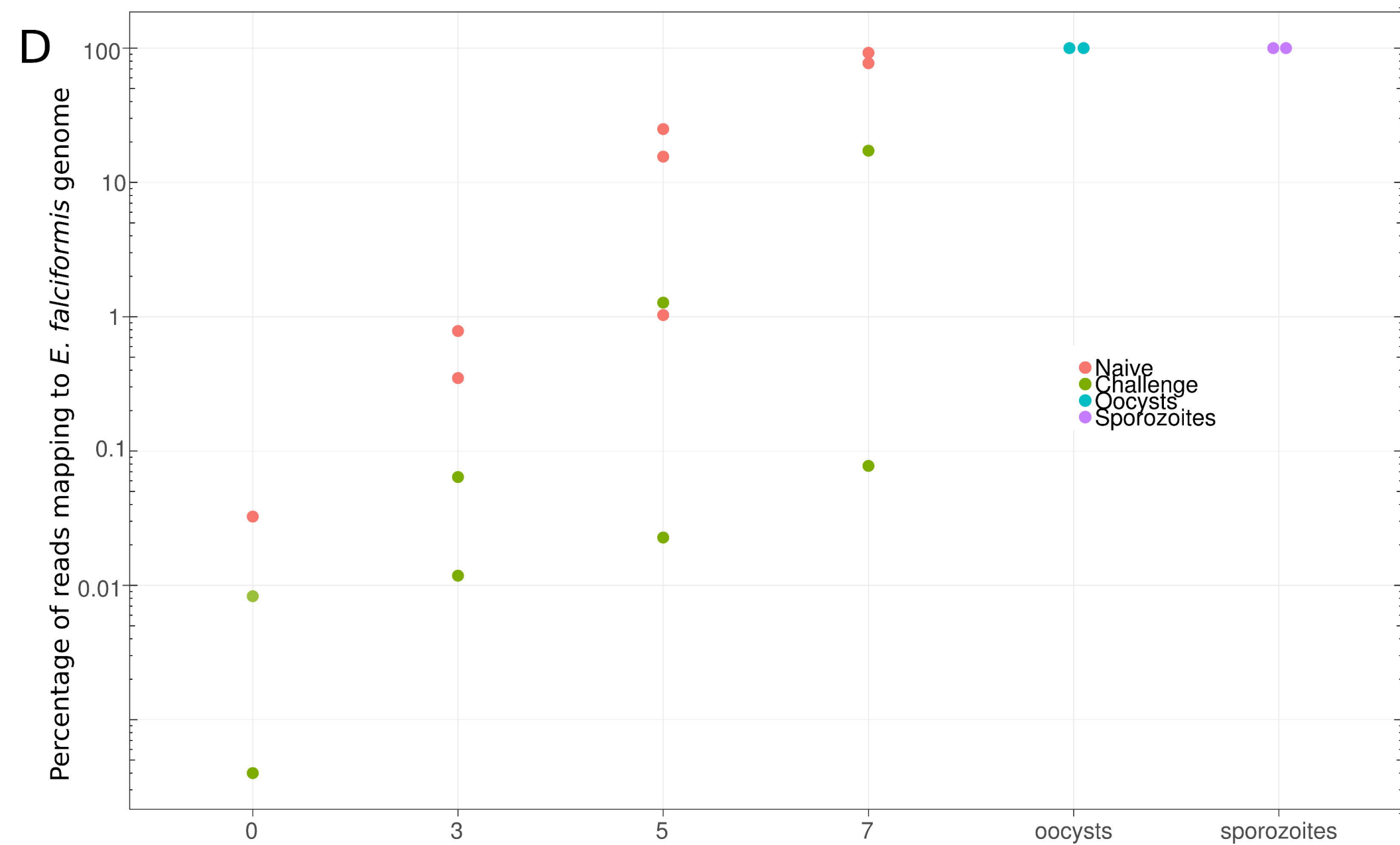
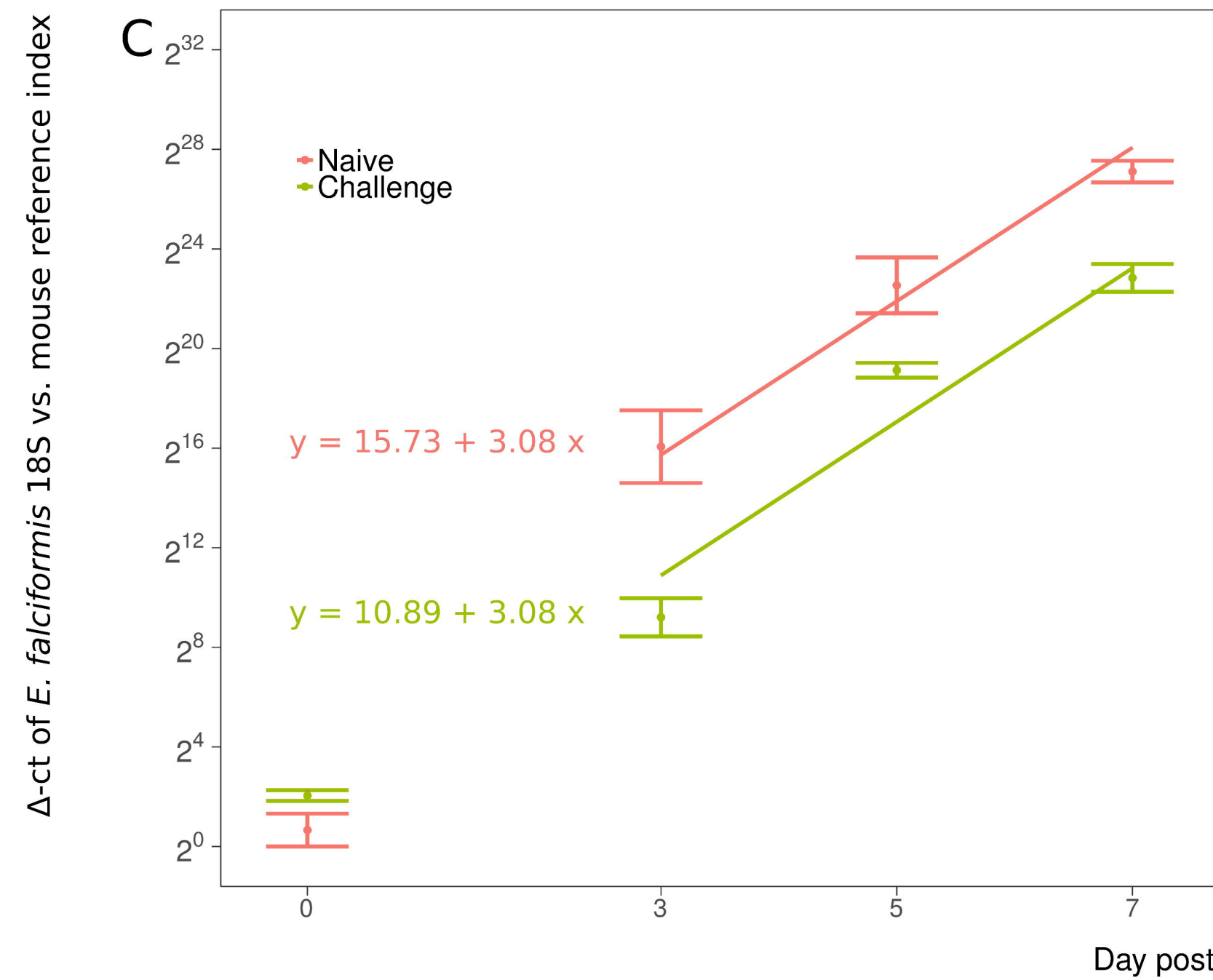
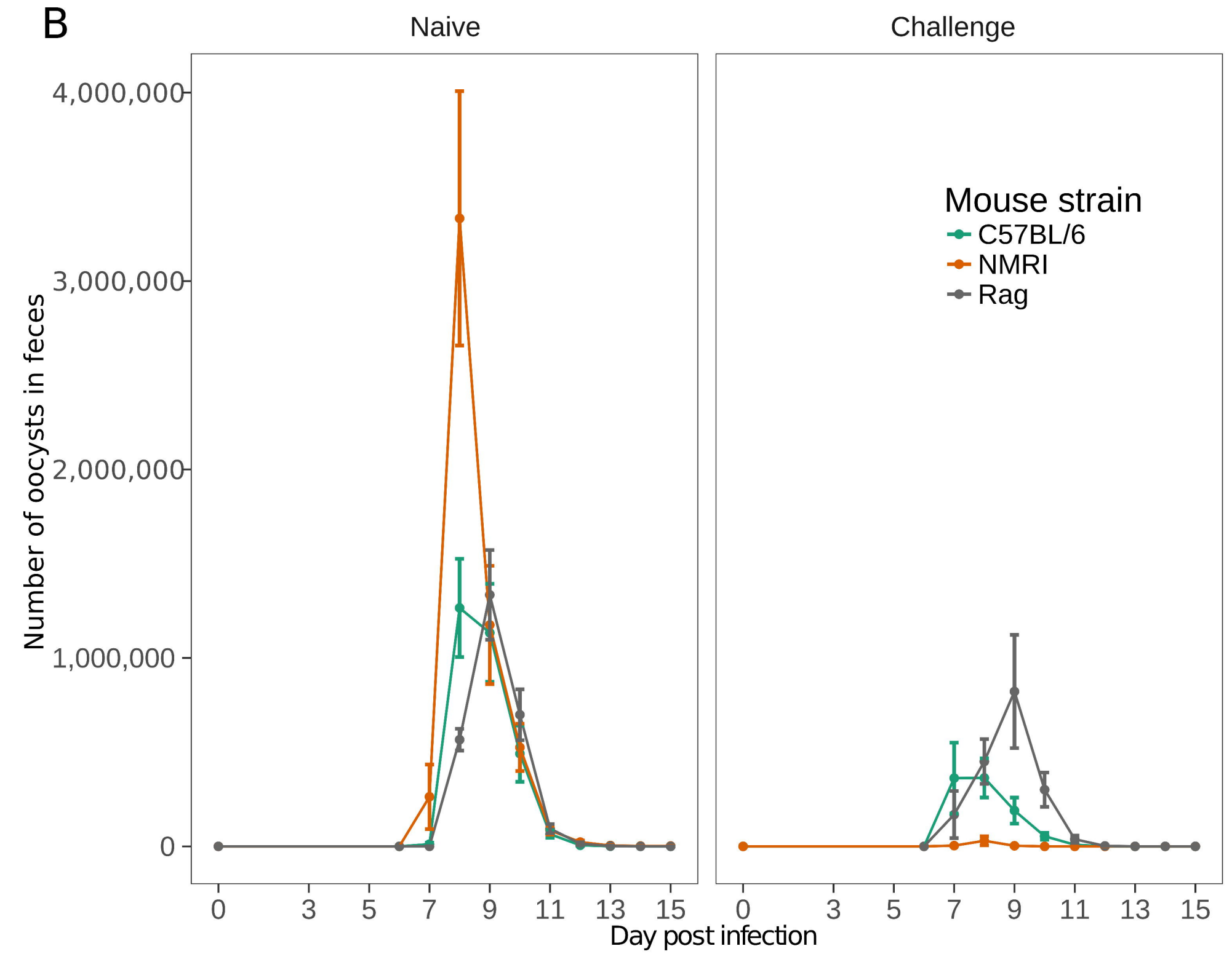
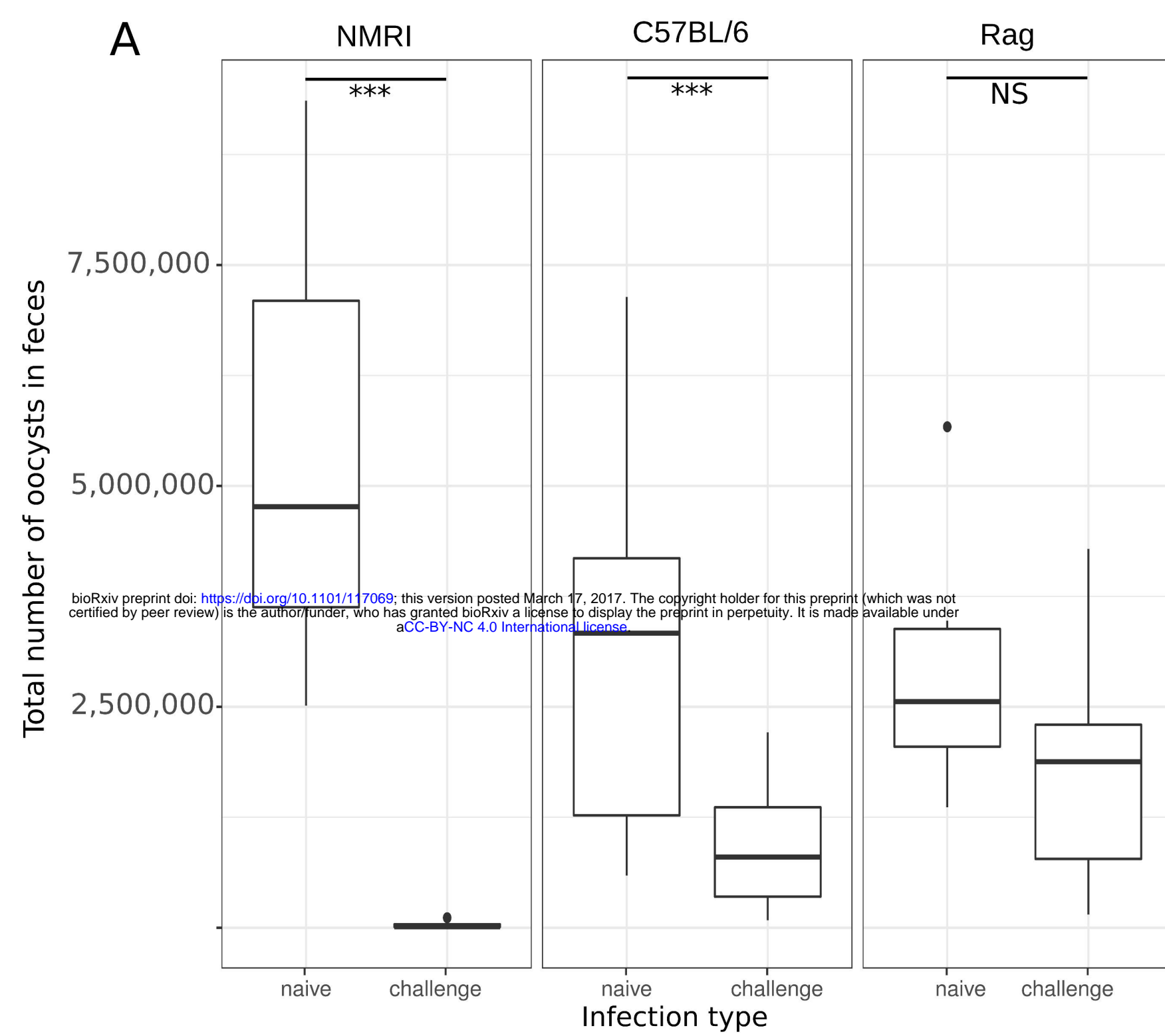
69. Trapnell C, Pachter L, Salzberg SL. TopHat: discovering splice junctions with RNA-Seq. *Bioinformatics.* 2009;25:1105–11.

70. Langmead B, Salzberg SL. Fast gapped-read alignment with Bowtie 2. *Nat. Methods.* 2012;9:357–9.

71. Liao Y, Smyth GK, Shi W. featureCounts: an efficient general purpose program for assigning sequence reads to genomic features. *Bioinformatics.* 2014;30:923–30.

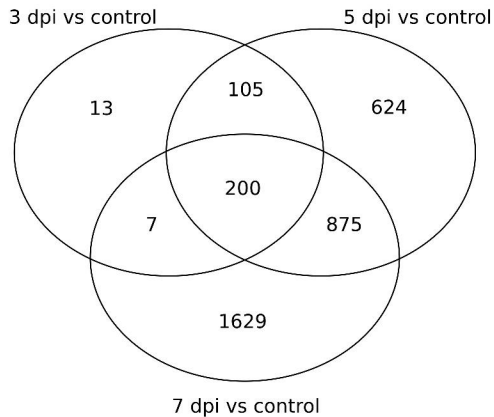
72. Robinson MD, McCarthy DJ, Smyth GK. edgeR: a Bioconductor package for differential expression analysis of digital gene expression data. *Bioinformatics.* 2010;26:139–140.

73. Benjamini Y, Hochberg Y. Controlling the false discovery rate: A practical and powerful approach to multiple testing. *J. R. Stat. Soc. Ser. B Methodol.* 1995;57:289–300.



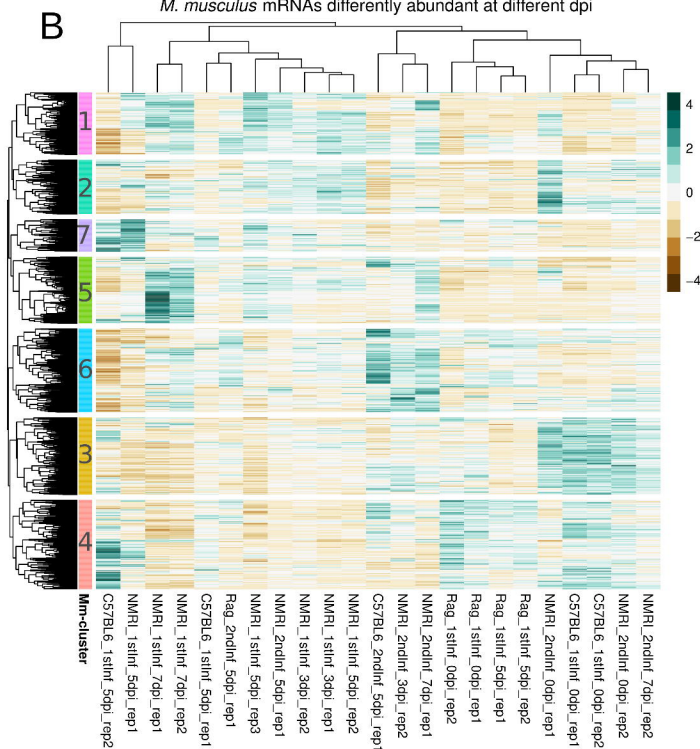
A

Differentially abundant mRNAs
between mouse groups

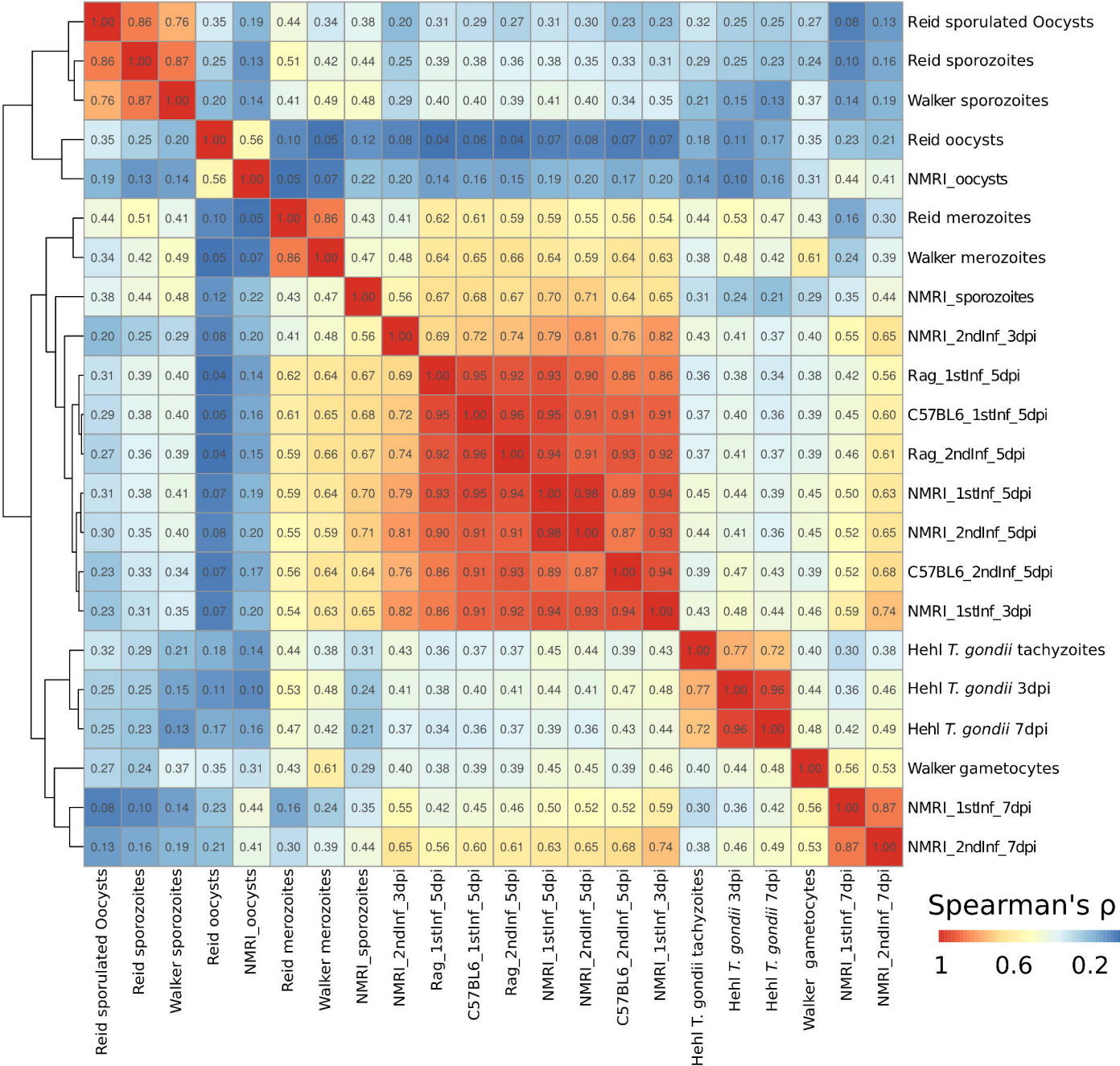


B

M. musculus mRNAs differently abundant at different dpi

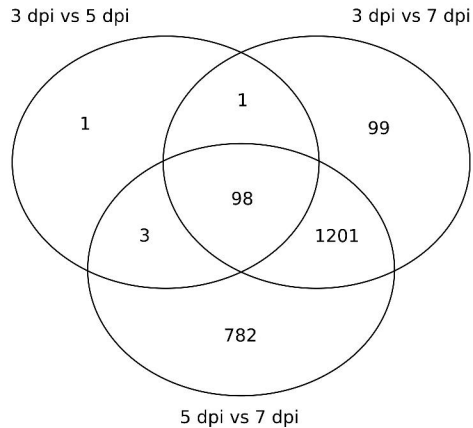


Correlation of mRNA abundance of orthologous genes from *E. falciformis*, *E. tenella* and *T. gondii* in different lifecycle stages



A

Differentially abundant mRNAs
between *E. falciformis* groups

**B**

E. falciformis mRNAs differently abundant at different dpi

